Hydrogen Bonding Interaction of Poly(D,L-Lactide)/hydroxyapatite Nanocomposites

Shaobing Zhou,* Xiaotong Zheng, Xiongjun Yu, Jianxin Wang, Jie Weng, Xiaohong Li, Bo Feng, and Ming Yin

School of Materials Science and Engineering, Key Laboratory of Advanced Technologies of Materials, Ministry of Education, Southwest Jiaotong University, Chengdu 610031, People's Republic of China

Received August 17, 2006. Revised Manuscript Received November 9, 2006

It was necessary to study the bonding mechanism of poly(D,L-lactide) (PDLLA) and hydroxyapatite (HA) nanoparticles because of their increasing application in medical fields. In this paper, hydrogen bonding between PDLLA and HA in PDLLA/HA nanocomposites was first investigated by scanning electron microscopy (SEM), differential scanning calorimetry (DSC), Fourier transform infrared spectroscopy (FTIR), and X-ray photoelectron spectroscopy (XPS). Structural morphology and glass transition temperature (T_g) of the nanocomposites showed that there was a close interaction between polymer matrix and inorganic nanoparticls. The results from FTIR and XPS indicated that the hydrogen bonding between the C═O in PDLLA and the surface P—OH groups of HA nanocrystalline was formed indeed. Shape memory properties were improved, which further implied the existence of hydrogen bonding in these nanocomposites. Thus, we designed a schematic model of the hydrogen bonding on the base of the experimental results. It can clearly explain the interaction mechanism of polymeric phases and inorganic phase in nanocomposites.

Introduction

Polylactide (PLA) that possesses biodegradation and biocompatibility has been approved by the U.S. Food and Drug Administration for application in clinical and pharmaceutical fields. It has been widely investigated for increasing applications as matrices for drug delivery systems,[1−4] bone implants, and bone fixation devices[5,6] and as three-dimensional scaffolds for tissue engineering[7] and surgical sutures.[8] HA ($Ca_{10}(PO_4)_6(OH)_2$) has been currently used in hard tissue engineering due to its excellent bioactivity, biocompatibility, and osteoconductivity.[9−11] However, the use of bulk HA is limited by its poor mechanical properties, such as low flexural strength and low fracture toughness.[12] The medical applications of biodegradable polymers (e.g., PLA, PGA, and their copolymers) are also limited due to their lower mechanical strength, toughness, and elastic modulus than those of natural cortical bones. Thus, for obtaining a desired material that holds high mechanical performance to match natural bones, nano-inorganic fillers were introduced into a polymer matrix to fabricate inorganic/polymeric composites, which has attracted wide attention.[13−17] Among them, PDLLA/HA nanocomposites have been used clinically in various forms[18,19] due to colligating their own advantages and overcoming their shortcomings. For example, the bone bonding ability of PLA/HA composite would be increased with the inclusion of HA.[20] Moreover, the modulus of the nanocomposite would be improved effectively with the introduction of HA into the PLA matrix.[21] The degradation kinetics of biodegradable polyesters and calcium phosphate/calcium carbonate in vitro pH studies has also been discussed.[22] However, the interaction mechanism between polymer and inorganic particles in composites was rarely explored.

Why do the nanocomposites possess better properties than single materials? It is well-known that the properties of materials are determined by their structure. Here, the reason that PLA/HA nanocomposites had excellent characteristics must also be the changed structures of PLA polymer matrix and HA in composites. We presumed that hydrogen bonding came into being between PLA and HA according to their

* To whom correspondence should be addressed. Phone: +86-28-87634023. Fax: +86-28-87634649. E-mail: shaobingzhou@home.swjtu.edu.cn or shaobingzhou@hotmail.com.

(1) Steendam, R.; Steenbergen, M. J.; Hennink, W. E.; Frijlink, H. W.; Lerk. C. F. *J. Controlled Release* **2001**, *70*, 71.
(2) Sarazin, P.; Roy, X.; Favis, B. D. *Biomaterials* **2004**, *25*, 5965.
(3) Liu, R.; Ma, G. H.; Meng, F. T.; Su, Z. G. *J. Controlled Release* **2005**, *103*, 31.
(4) Edlund, U.; Albertsson, A. C. *Adv. Polym. Sci.* **2000**, *157*, 68.
(5) Leclerc, E.; Furukawa, K. S.; Miyata, F.; Sakai, Y.; Ushida, T.; Fujii, T. *Biomaterials* **2004**, *25*, 4683.
(6) Leiggener, C. S.; Curtis, R.; Muler, A. A.; Pfluger, D.; Gogolewski, S.; Rahn, B. A. *Biomaterials* **2006**, *27*, 202.
(7) Richardson, S. M.; Curran, J. M.; Chen, R.; Thomas, A. V.; Hunt, J. A.; Freemont, A. J.; Hoyland, J. A. *Biomaterials* **2006**, *27*, 4069.
(8) Rokkanen, P. *Biomaterials* **2000**, *21*, 2607.
(9) Kokubo, T.; Kim, H. M.; Kawashita, M. *Biomaterials* **2003**, *24*, 2161.
(10) Hench, L. L. *J. Am. Ceram. Soc.* **1998**, *81*, 1705.
(11) Jarcho, M. *Clin. Orthop.* **1981**, *157*, 259.
(12) Tancred, D. C.; McCormack, B. A.; Carr, A. J. *Biomaterials* **1998**, *19*, 1735.
(13) Shikinami, Y.; Okuno, M. *Biomaterials* **1999**, *20*, 859.
(14) Shikinami, Y.; Okuno, M. *Biomaterials* **2001**, *22*, 3197.
(15) Choi, D.; Marra, K. G.; Kumta, P. N. *Mater. Res. Bull.* **2004**, *39*, 417.
(16) Liu, Q.; de Wijn, J. R.; van Toledo, M.; Bakker, D.; van Blitterswijk, C. A.; Mate, J. *Sci. Mater. Med.* **1998**, *9*, 23.
(17) Choi, D.; Marra, K. G.; Kumta, P. N. *Mater. Res. Bull.* **2004**, *39*, 417.
(18) Liao, S. S.; Cui, F. Z.; Zhang, W.; Feng, Q. L. *Biomed. Mater. Res. Part B* **2004**, *69*, 158.
(19) Kim, S. S.; Park, M. S.; Jeon, O.; Choi, C. Y.; Kim, B. S. *Biomaterials* **2006**, *27*, 1399.
(20) Yasunaga, T.; Matsusue, Y.; Furukawa, T.; Shikinami, Y.; Okuno, M.; Nakamura, T. *J. Biomed. Mater. Res.* **1999**, *47*, 412.
(21) Kasuga, T.; Ota, Y.; Nogami, M.; Abe, Y. *Biomaterials* **2001**, *22*, 19.
(22) Schiller, C.; Epple, M. *Biomaterials* **2003**, *24*, 2037.

10.1021/cm0619398 CCC: $37.00
Published on Web 12/20/2006

functional groups analysis. The hydrogen bond is really a special case of dipole forces. A hydrogen bond is the attractive force between the hydrogen attached to an electronegative atom of one molecule and an electronegative atom of a different molecule. Hydrogen bonding is crucial in many chemical and biochemical reactions as well as in determining material properties. Now the research of it focuses on small molecules such as H_2O and some biomacromolecules (e.g., DNA).[23,24] However, to the best of our knowledge, little literature has reported the bonding mechanism between PLA and HA. Some researchers mentioned that PLLA was directly grafted onto the hydroxyl group of the surface of nano-HA particles by ring-opening polymerization of L-lactide.[25] In fact, the ring-opening reaction was initiated by the hydroxyl groups of the surface of HA particles, and the connected chemical bonding was assumed as ionic bonding. Kasuga et al. also mentioned that the carbonyl group of the PLA can form weak ionic bonds with calcium in the HA.[21] Some papers have only reported that hexanoic and decanoic acids molecules were hydrogen bonded to the surface P—OH groups of HA[26] and that adsorption of organic bases was due to the formation of surface hydrogen bonds between their nitrogen atoms and the P—OH groups of hydroxyapatite.[27] The formation of hydrogen bonding of PDLLA and HA in previous literature has hardly been addressed.

Currently the crystal structure question under continuous experimental and theoretical research is related to the hydroxylation on the real crystal structure of biological apatites.[28] There is no complete consensus on the FTIR spectra sites of the surface P—OH groups in HA crystal. Cheng et al. thought that the peaks of the surface P—OH groups should be in the range of 3650−3680 cm^{-1}.[29] These peaks around 2100 cm^{-1} were most likely due to P—OH vibrational modes reported by Nicholas et al.[30] Hence, for solving these questions, in the paper, we also selected nanocrystalline HA as a filler to prepare PDLLA/ HA nanocomposites with different weight ratios. The dispersed morphology and T_g of composites were examined by SEM and DSC, respectively. The spectra of the surface P—OH groups were clearly discussed by FTIR. Moreover, the formation of hydrogen bonding between carbonyl in PDLLA and the surface hydroxyl in nanocrystal HA was analyzedby FTIR and XPS. The shape memory properties of nanocomposites were also investigated in order to further evaluate the formation of hydrogen bonding.

Experimental Section

Materials. PDLLA (the average molecular mass, M_w 152 kDa) was synthesized by ring-opening polymerization of the D,L-lactide monomer.[31] The molecular weight distribution was 1.57 as determined by Waters 2695/2414 gel permeation chromatography (GPC, Waters, U.S.). The nanocrystalline HA was prepared by a wet chemical method at low temperature in an aqueous medium.[32] The average size of 78 nm and the size distribution from 50 to 90 nm were determined by laser diffraction particle size analyzer (Malven, Mastersizer 2000, UK) and the molar ratio of Ca/P = 1.62 was determined by chemical analysis. All other chemical reagents were of reagent grade and used as received.

Preparation of PDLLA/HA Nanocomposites. The PDLLA/HA nanocomposites were prepared at weight ratios of 1:1, 2:1, and 3:1 as in our previous report.[33] The only difference is in the final step, namely, those completely dried composites were press-molded at 105 °C for 10 min in a mold that was designed to a film shape, and the pressing was performed in the pressure range of 10−15 MPa. Thus, we could obtain specimens with a film shape at weight ratios of 1:1, 2:1, and 3:1.

Characterization of the Nanocomposites. The surface morphology was observed using a Quanta200 scanning electron microscope (SEM, FEI, U.S.). Pieces of the specimens were mounted and then coated with gold. The accelerating voltage and magnification was 20 keV and 60 000×, respectively.

STA 449C differential scanning calorimetry (DSC, NETZSCH, Germany) was use to detect the T_g of pure PDLLA and the nanocomposites. The specimens were heated from 10 to 110 °C at a rate of 5 °C/min in flowing nitrogen gas. Weights of all samples were from 5 to 8 mg.

Nicolet 5700 FTIR spectroscopy (Thermo Electron, U.S.) was performed to identify the changes of some functional groups in PDLLA/HA composites as compared with pure PDLLA and HA. All specimens were made into particles and mixed with KBr grains at a weight ratio of 0.5−1%. Pure KBr was used as IR spectral reference, and each sample was recorded from 4000 to 400 cm^{-1} by 64 scans.

The chemical composition of elements was analyzed by ESCALAB Mark II X-ray photoelectron spectroscopy (XPS, VG Scientific, UK) using monochromatic Mg Kα radiation (1253.6 eV) from the Mg anode source. The binding energy (BE) was referenced to at 284.6 eV to the C 1s peak, and the high-resolution scans of core level spectra were set to 15 eV pass energy and recorded with an energy step of 0.05 eV. All obtained experimental data were deconvolved by Gaussian−Lorentzian mixture peak-fitting software.

Investigation of Shape Recovery Ratios on PDLLA/HA Nanocomposites. These interesting shape recovery behaviors of pure PDLLA and PDLLA/HA nanocomposites with weight ratios of 3:1, 2:1, and 1:1 were investigated.

(23) Jeffrey, G. A. *An Introduction to Hydrogen Bonding*; Topics in Physical Chemistry; Oxford University Press: New York, 1997; ISBN 0195095499.
(24) Crabtree, H. R.; Siegbahn, P. E. M.; Eisenstein, O.; Rheingold, A. L. Koetzle, T. F. *Acc. Chem. Res.* **1996**, *29* (7), 348.
(25) Hong, Z. K.; Qiu, X. Y.; Sun, J. R.; Deng, M. X.; Chen, X. S.; Jing, X. B. *Polymer* **2004**, *45*, 6699.
(26) Tanaka, H.; Watanabe, T.; Chikazawa, M.; Kandori, K.; Ishikawa, T. *J. Colloid Interface Sci.* **1999**, *214*, 31.
(27) Nikolenko, N. V.; Esajenko, E. E. *Adsorpt. Sci. Technol.* **2005**, *23*, 543.
(28) Leventouri, T. *Biomaterials* **2006**, *27*, 3339.
(29) Cheng, Z. H.; Yasukawa, A.; Kandori, K.; Ishikawa, T. *Langmuir* **1998**, *14*, 6681.
(30) Nicholas, L. B.; Wilson, O. C., Jr. *Biomaterials* **2003**, *24*, 3671.
(31) Deng, X. M.; Zhou, S. B.; Li, X. H.; et al. *J. Controlled Release* **2001**, *71*, 165.
(32) Murugan, R.; Ramakrishna, S. *J. Cryst. Growth* **2005**, *274*, 209.
(33) Zheng, X. T.; Zhou, S. B.; Li, X. H.; Weng, J. *Biomaterials* **2006**, *27*, 4288.

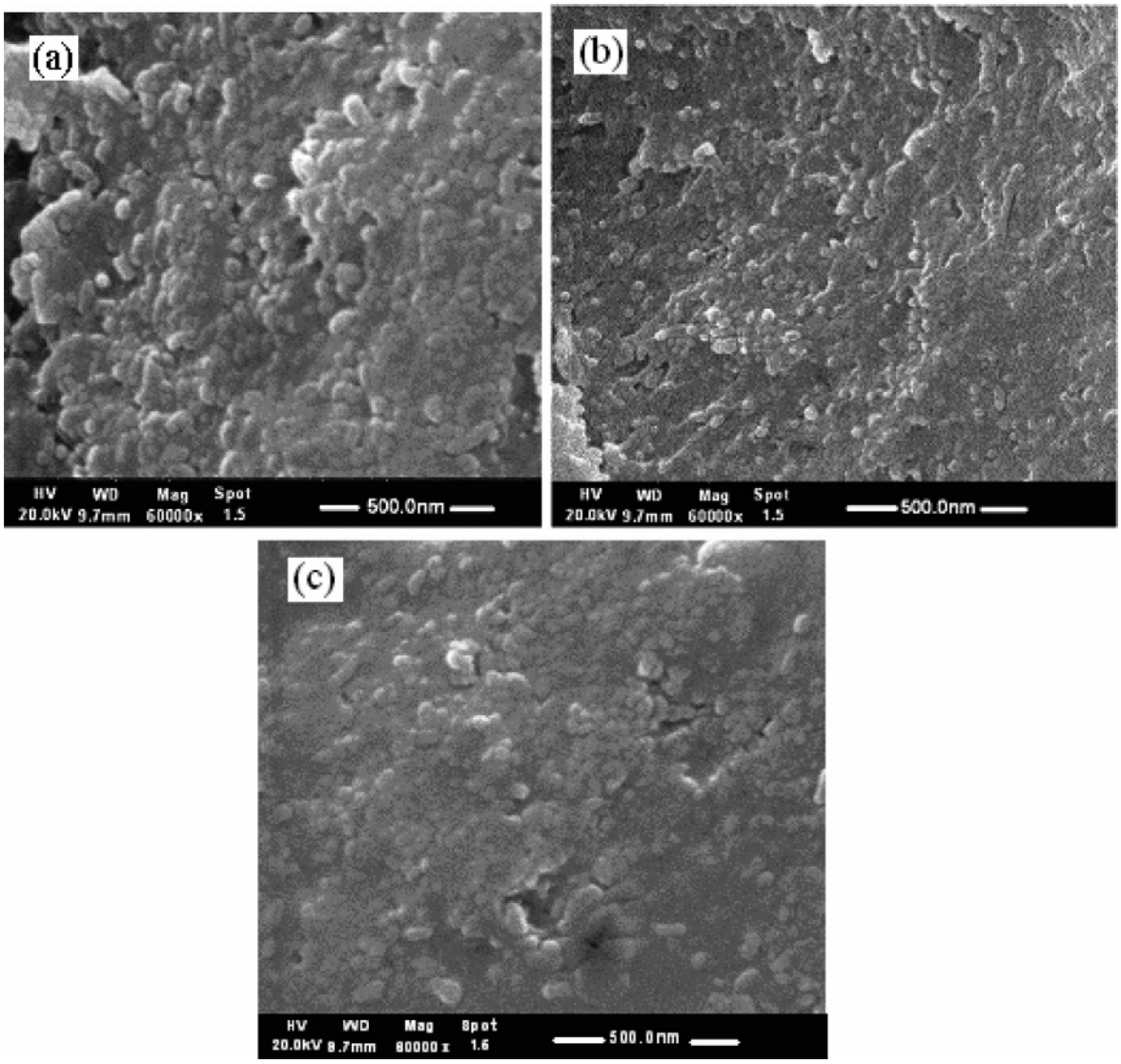

Figure 1. SEM micrographs for PDLLA/nano-HA composites at a (a)1:1, (b) 2:1, (c) 3:1 weight ratio.

All samples with size of 10 × 5 × 1 mm (length × width × thickness) were deformed at 70 °C and recovered at 74 °C, as in our previous report.[33] Shape recovery ratios of all samples were tested.

Results and Discussion

Morphology of PDLLA/HA Nanocomposites. Figure 1 shows SEM images of PDLLA/HA nanocomposites with weight ratios of 1:1, 2:1, and 3:1 upon high magnification of 60 000×. As seen from Figure 1, we can find that it is evident that HA nanoparticles are completely uniformly distributed in the polymer matrix. It also indicates that there are a few agglomerations of nanocrystals in PDLLA matrix by the blend method. Therefore, HA nanoparticles can yet keep general nanoeffects in the nanomposites. In addition, although it cannot be proven what bonding the interface of two phases is, it can indicate that the uniform contact is not simply a physical bonding because the chemical action contributes to prevent agglomeration of nanopowders.[34]

(34) Shan, H. B.; Zhang, Z. T. *J. Eur. Ceram. Soc.* **1997**, *17*, 713.

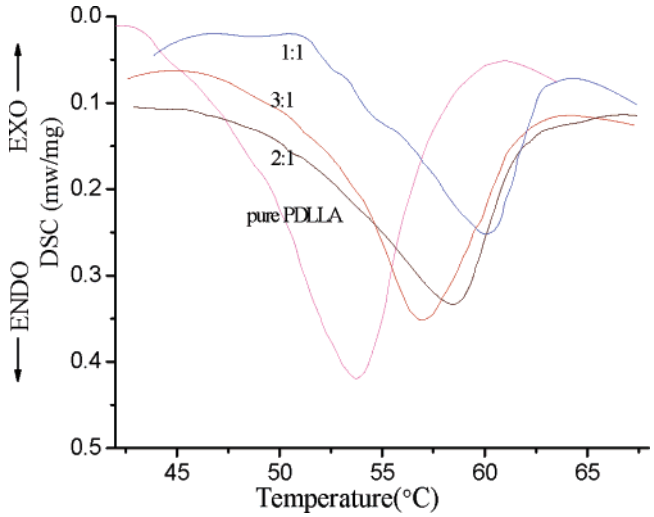

Figure 2. DSC thermograms of pure PDLLA and PDLLA/HA composites at a weight ratio of 1:1, 2:1, and 3:1.

***T_g* of PDLLA/nano-HA.** In order to further investigate the bonding between the two phases, DSC was employed. Figure 2 shows the DSC heating curves of pure PDLLA and PDLLA/HA nanocomposites with weight ratios of 3:1, 2:1,

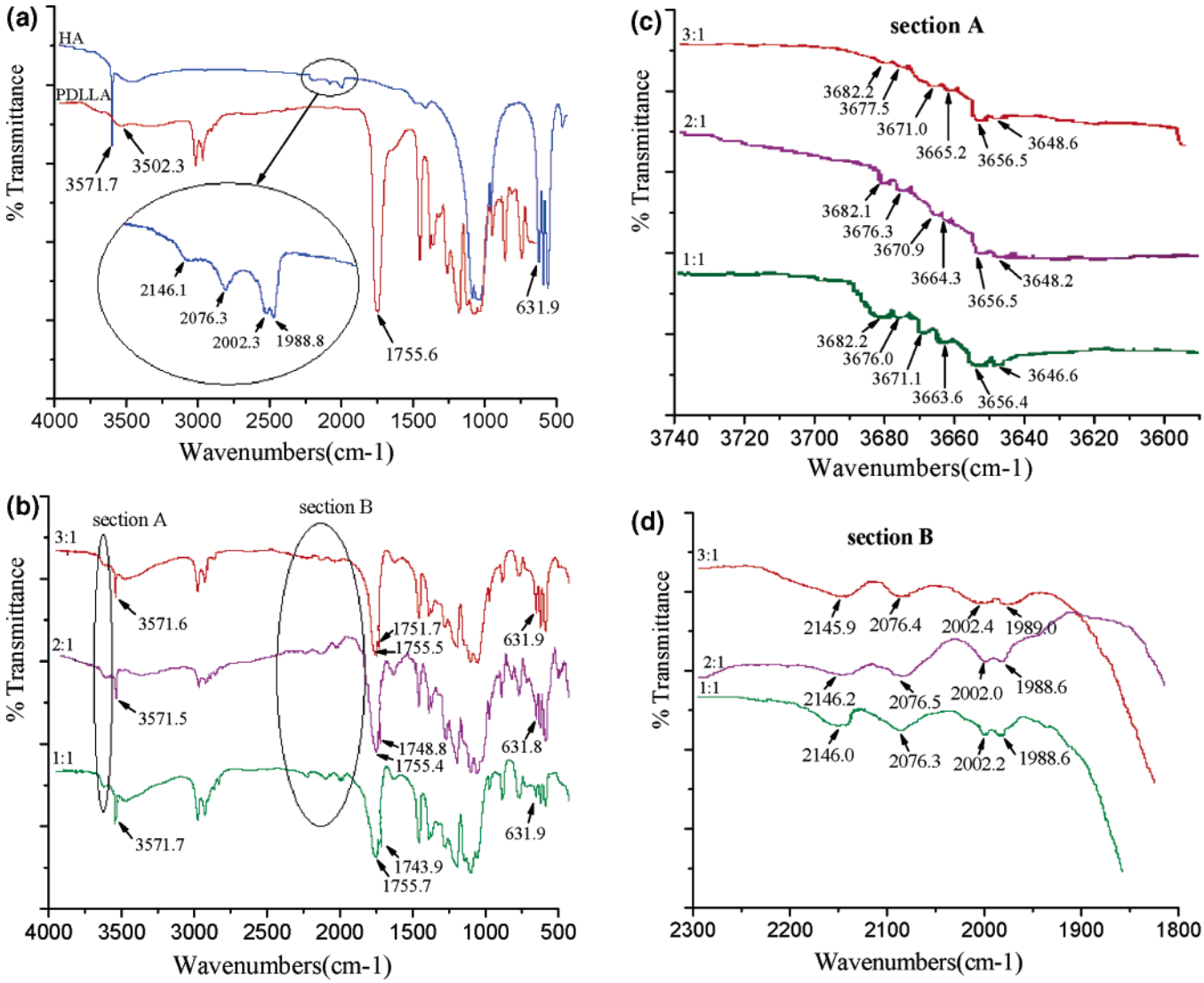

Figure 3. FTIR spectra of pure PDLLA and HA nanoparticles (a), PDLLA/HA nanocomposites at a weight ratio of 3:1, 2:1,1:1 (b), magnified FTIR spectra of PDLLA/HA nanocomposites at section A (c), and magnified FTIR spectra of the nanocomposites at section B (d).

and 1:1. The amorphous PDLLA presents an endothermic peak, namely T_g, heating from glassy state to rubbery state, and the T_g is 53.8 °C. HA in composite has no polymeric T_g, so the endothermic peak should attribute to PDLLA, as shown in Figure 2. It can be seen that T_g of the composites at a weight ratio of 3:1, 2:1, and 1:1 are 56.8, 58.7, and 60.1 °C, respectively. Moreover, the T_g increased with the increase of HA concentration in the matrix. One reason may be that the micro-Brownian thermal motions of molecular chains of PDLLA were constrained by HA nanoparticles during endothermic process. Another reason may be that the existence of interfacial interaction of the two phases provided an increase in the polymeric T_g.[35] Thus, the DSC thermogram also indicated that there was chemical bonding between PDLLA and nano-HA, which was in agreement with the results of the SEM images.

FTIR Analysis of Hydrogen Bonding. In order to know which bonding occurred between the two phases, FTIR was used. The IR spectra of pure PDLLA and nanocrystalline HA are presented in Figure 3a. From the curve of PDLLA, it can be observed that there is a strong absorption band at 1755.6 cm^{-1} where, corresponding to the carbonyl group (C═O), the bands at 2994.1 and 2876.0 cm^{-1} are assigned to the C−H stretching vibrations of CH_3 groups in the side chains. Similarly, the bands at 2944.3 and 2847.0 cm^{-1} are attributed to the −CH− groups in the stem chains of PDLLA. There a band can be seen at 3502.3 cm^{-1}, which should be assigned to terminal hydroxyl groups (−OH) of PDLLA.[36] Figure 3a also shows the IR spectrum of nano-HA. It is consensus on the sharp bands at 3571.7 and 631.9 cm^{-1} due to OH− stretching and bending modes in crystal lattice of HA, respectively. Near a broad peak at 3432.5 cm^{-1} is related to adsorbed H_2O.[37] The peaks of PO_4^{3-} ions have four vibration spectra (namely, υ_1, υ_2, υ_3, and υ_4). The υ_1 peak is present at 962.1 cm^{-1}, the υ_2 peak is observed at 472.7 cm^{-1}, the board υ_3 peak is shown at 1090.2 and 1047.1 cm^{-1}, and the sharp peaks at 601.8 and 570.5 cm^{-1} are attributed to υ_4 vibration mode. It is noted that there are doublet peaks at 1477.6 and 1411.3 cm^{-1} attributed to CO_3^{2-} vibration, which

(35) Young, S. K.; Gemeinhardt, G. C.; Sherman, J. W.; Storey, R. F.; Mauritz, K. A.; Schiraldi, D. A.; Polyakova, A., Hiltner, A., Baer, E. *Polymer* **2002**, *43*, 6101.

(36) Gonsalves, K. E.; S. Jin, M. I. *Biomaterials* **1998**, *19*, 1501.

(37) Ishikawa, T.; Wakamura, M.; Kondo, S. *Langmuir* **1989**, *5*, 140.

is a Ca-deficient B-type carbonate ion occupying the vertical face of the substituted phosphate ion.[38,39] The crystal structure of B-type carbonate apatite has kept the problem unresolved,[28] but the origin of CO_3^{2-} in HA is CO_2 dissolved from air into the solutions during the preparation.[29] The IR spectra in the elliptic frame shown in Figure 3a are related to P—OH or PO_4^{3-} groups of HA crystal at 2146.4, 2076.3, 2002.3, and 1988.8 cm^{-1}, respectively. Nicholas et al. attributed these peaks around 2100 cm^{-1} to P—OH vibration modes.[30] More researchers[29,37,40] thought that the peaks of the surface P—OH groups should be in the range of 3650—3680 cm^{-1}, which was not present in Figure 3. For verifying these different opinions, we will discuss it from the IR spectral results shown in Figure 3b—d.

Figure 3b shows the IR spectra of PDLLA/HA nanocomposites at weight ratios of 3:1, 2:1, and 1:1. As seen in the figure, in the nanocomposites the stretching vibrations of C═O were all split up into two peaks as compared to the carbonyl peak of pure PDLLA. One peak at about 1755 cm is assigned to the original C═O vibration of PDLLA, which is free and is not bonding with HA nanoparticles; the other takes blue-shift obviously, which ascribed to the interaction of PLA and HA. Moreover, the phenomena of blue-shift of the C═O becomes more obvious with the increase of nano-HA particles addition. It indicates that nano-HA plays an important role in presence of the new C═O vibration peak and there exists hydrogen bonding between the carbonyl group of PDLLA and another active group in composite. On the other hand, all composites have other new peaks shown in section A of Figure 3b. From the magnified spectra of composites at section A shown in Figure 3c, many weak peaks can be observed. According to previous literature,[29,37,40] several peaks at about 3682, 3671, and 3656 cm^{-1} are assignable to P—OH vibration modes. Other peaks, which were not mentioned in previous literature, could also attribute to the P—OH groups resulting in the chemical action in composites for the FTIR spectra of composites beyond 3500 cm^{-1} are all attributed to —OH stretching vibration modes.[25,36,37,41]

XPS Analysis of Hydrogen Bonding. From the above discussion, it is possible that hydrogen bonding existed in PDLLA/nano-HA composite by the bonding connection of the surface P—OH group of nano-HA and C═O group of PDLLA. The change in binding energy (BE) of chemical bonds was further investigated and evaluated by XPS analysis.

Figure 4 shows the XPS spectra of C 1s (a) and O 1s (b) core level spectra of pure PDLLA; P 2p (c), O 1s (d), and Ca 2p (e) core level spectra of nanocrystalline HA; and C 1s (f), O 1s (g), P 2p (h), and Ca 2p (i) core level spectra of PDLLA/HA composites at a weight ratio of 3:1, 2:1, and 1:1. Carbon signals of the three components shown in Figure 4a are displayed to three different binding energies at 284.75, 286.04, and 288.64 eV, which are attributed to —***C***H_3 in side chain, —***C***H, and ***C***═O in stem chain, respectively.[42] Similarly, Figure 4b shows that the two fitting peaks of oxygen bonds at 531.73 and 532.97 eV are assigned to ***O***—C and ***O***═C, respectively. Figure 4c,d shows that the spectrum of P 2p bond at 133.48 eV results from the ***P***O_4^{3-} group of HA, and the O 1s spectrum at 530.98 eV is assigned to the phosphate oxide.[43,44] Figure 4e shows that the Ca 2p core level presents the doublet bonds at a BE of 374.32 and 351.10 eV, which should attribute to $2p_{3/2}$ and $2p_{3/2}$ of Ca 2p orbit.[44,45] By comparing with BE of every element for pure PDLLA and HA, we can find that the C 1s BE of ***C***═O in PDLLA of three composites at a weight ratio of 3:1, 2:1, and 1:1 shifted to 288.72, 288.81, and 288.89 eV, respectively (Figure 4f). From Figure 4g, it is observed that the O 1s BE of ***O***═C in the three nanocomposites shifted from 532.97 eV to 533.08, 533.13, and 533.20 eV, respectively. Moreover, new peaks at 531.49, 531.46, and 531.41 eV were respectively detected, which may be assigned to the O 1s BE of the surface P—***O***H group in PDLLA/HA composites.[46] From Figure 4h,i, we also find that the P 2p BE and Ca 2p BE in all composites took changes. It can be seen that the C 1s and O 1s BE of C═O increase and that P 2p, Ca 2p, and O 1s BE of phosphate decrease as the addition of nano-HA particles increase. The reason should be attributable to the formation of hydrogen bonding between the C═O in PDLLA and the OH on the surface of HA nanoparticles.

The interaction mechanism of hydrogen bonding is the electron attraction between a proton donor and a proton acceptor. XPS spectra of hydrogen bonding between C═O and OH groups represent that the O 1s BE of the C═O groups increases because of the electron transfer from the C═O groups to the OH groups, and the O 1s BE of the OH groups decreases due to the increase in the electron density.[47] Based on the theory, we find that the O 1s BE of the C═O groups in composites shifted to higher value (Figure 4 g), even though it cannot be confirmed that the O 1s BE of the surface P—OH groups in composites shifted to a lower value for no O 1s spectra of the P—OH group occurs in nano-HA (Figure 4d). The P 2p BE in composite decreased as compared to the value in pure HA, which indicates that the surface P—OH BE has shifted to the lower value. Therefore, the different changes of the O 1s of C═O and P—OH groups in the composites can be deduced that the formation of hydrogen bonding between the C═O group in PDLLA and the surface P—OH group in nano-HA. The C 1s BE of C═O group comparing to pure PDLLA increases and the Ca 2p BE of phosphate ion corresponding to HA crystal decreases, which also strongly confirms the formation of hydrogen bonding in the composite. The analyzed results of

(38) Ivanova, T. I.; Kamenetskaya, O. V. F.; Kol'tsov, A. B.; Ugolkov, V. L. *J. Solid State Chem.* **2001**, *160*, 340.
(39) Fleet, M. E.; Liu, X. *J. Solid State Chem.* **2004**, *177*, 3174.
(40) Tanaka, H.; Yasukawa, A.; Kandori, K.; Ishikawa, T. *Langmuir* **1997**, *13*, 821.
(41) Ignjatovic, N.; Savic, V.; Najman, S.; Plavsic, M.; Uskokovic, D. *Biomaterials* **2001**, *22*, 571.
(42) Kiss, E.; Bertoti, I.; Butler, E. I. V. *J. Colloid Interface Sci.* **2002**, *245*, 91.
(43) Yan, L. L.; Leng, Y.; Weng, L. T. *Biomaterials* **2003**, *24*, 2585.
(44) Nishikawa, H. *J. Mol. Catal. A: Chem.* **2003**, *206*, 331.
(45) Gopinath, C. S.; Hegde, S. G.; Ramaswamy, A. V.; Mahapatra, S. *Mater. Res. Bull.* **2002**, *37*, 1323.
(46) Kaciulis, S.; Mattogno, G.; Pandolfi, L.; Cavalli, M.; Gnappi, G.; Montenero, A. *Appl. Surf. Sci.* **1999**, *151*, 1.
(47) Li, L.; Chan, C. M.; Weng, L. T. *Polymer* **1998**, *39*, 2355.

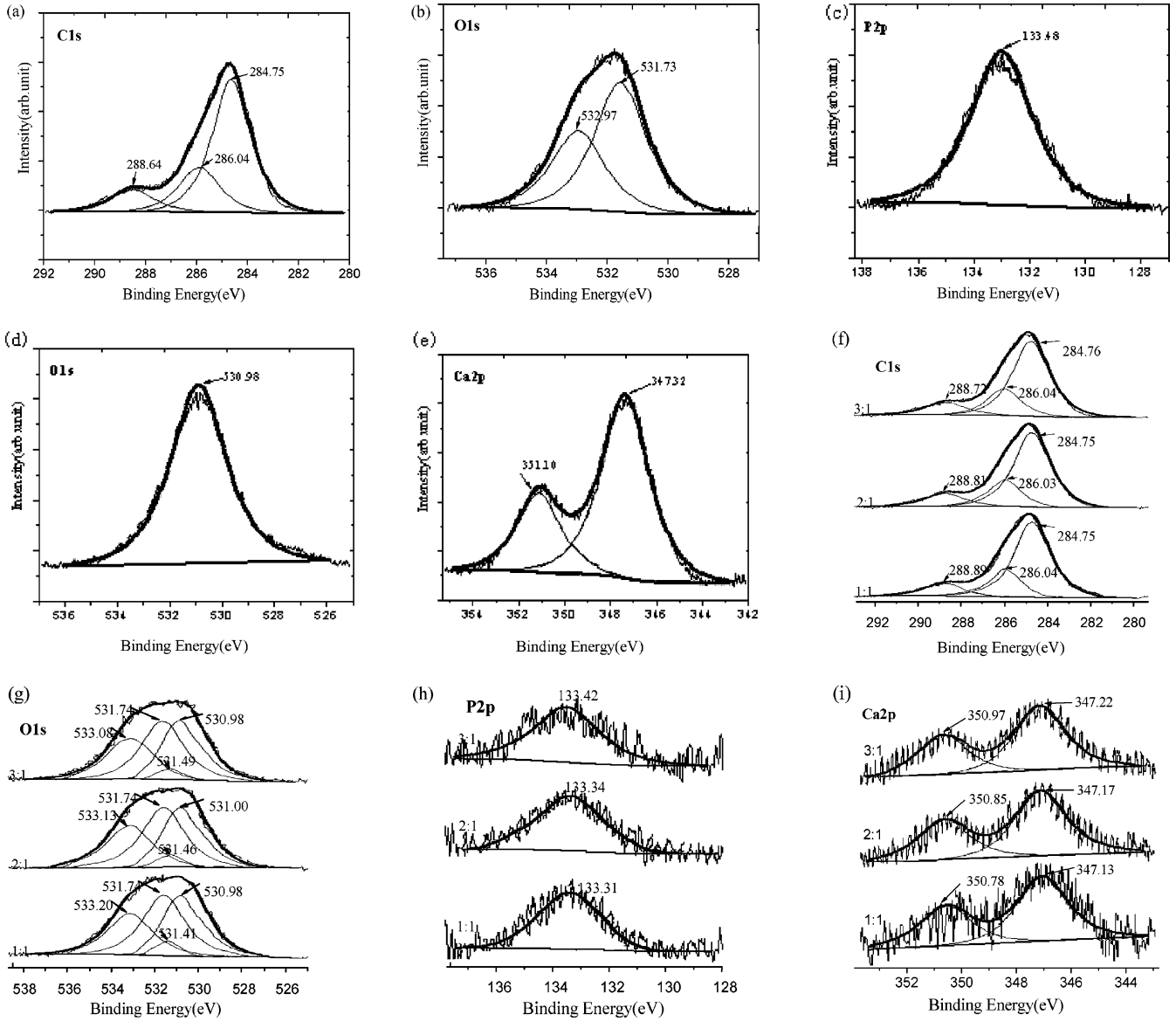

Figure 4. XPS of C 1s (a) and O 1s (b) core level spectra of pure PDLLA, and P 2p (c), O 1s (d), and Ca 2p (e) core level spectra of nanocrystalline HA and C 1s (f), O 1s (g), P 2p (h), and Ca 2p (i) core level spectra of PDLLA/HA composites at a weight ratio of 3:1, 2:1, and 1:1.

Figure 5. Photos show the process of shape memory recovery of a sample made of PDLLA/HA composite at a weight ratio of 3:1 taken with digital camera.

XPS spectra are also completely in accordance to that of FTIR spectra.

Interface Analysis of Shape Memory Properties. In order to explain the existence of hydrogen bonding in the nanocomposites more clearly, the shape memory properties of pure PDLLA and all nanocomposites were investigated as our previous report.[33] We illustrated a very interesting shape recovery behavior for a typical PDLLA/HA nanocomposite at a weight ratio of 3:1. As shown in Figure 5, the photos for the full process of shape memory recovery were taken at different times. When the deformed sample was heated at 74 °C over its T_g again, it started to recover shape immediately. The deformed sample recovered basically to original shape at the 60th second. The final shape recovery ratio (R) of all samples was calculated by the following formula:

$$R = \frac{L_d - L_f}{L_d - L_o} \times 100\%$$

where L_o, L_d, and L_f are the original length, the deformed length, and the final recovery length of sample, respectively (marked in Figure 5). The calculated result shows that the R values of all composites are over 98%, whereas R of pure PDLLA is only 80.5%. The results indicated that PDLLA/HA nanocomposite had well-shaped memory effect as compared to pure PDLLA.

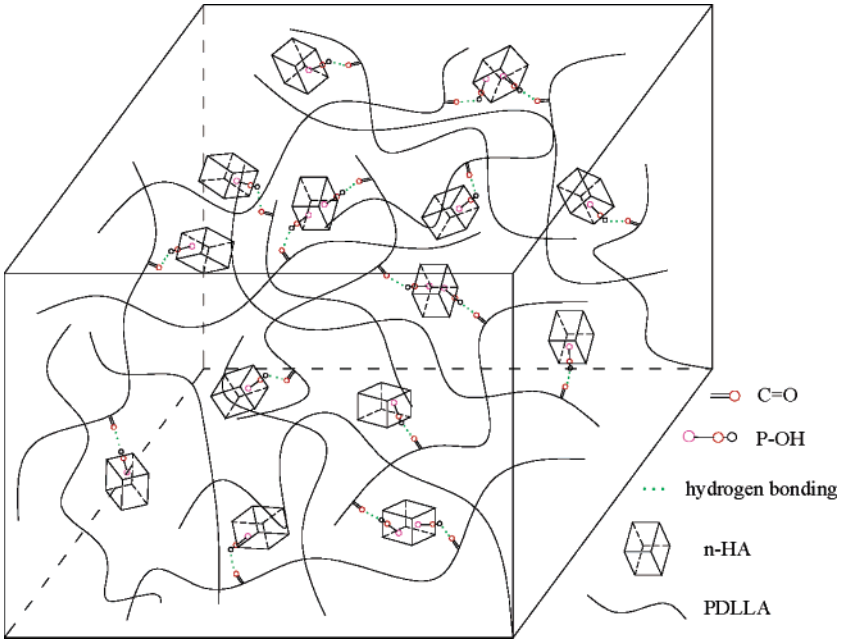

Figure 6. Schematic model of hydrogen bonding between C═O groups in PDLLA and the surface P—OH groups in HA nanoparticles.

The mechanism of shape memory effect in polymers may be that thermoplastic shape memory polymers have at least two separated phases, namely, stationary phase and reversible phase, where the domains with the highest thermal transition stabilize the permanent shape and a second phase having another thermal transition serves as switch.[48,49] The shape fixity of amorphous PDLLA polymer depends on a random winding of molecular chains. Thus, amorphous PDLLA polymer with a random winding as stationary phase has a low *R*. However, the shape memory effect of PDLLA/HA nanocomposite is improved obviously. So it is further indicated that there was physical crosslinking by connection of hydrogen bonding between HA and PDLLA. The amorphous PDLLA polymer in the composite was selected as reversible phase and the physical crosslinking between PDLLA and HA nanoparticle was acted as stationary phase. In conclusion, the reasons can be that the pure PDLLA is amorphous polymer and there is unsteady stationary phase by a random winding in polymer matrix.[50] However, shape memory effect of the pure PDLLA can be improved by compounding with HA particles while the steady stationary phase and reversible phase came into being.[33] On the other hand, it should be noticed that the shape recovery properties of the PDLLA/HA nanocomposites did not completely increase with the increase of the HA particles, which were the best at definite range of compound ratio due to increasing constraint of the micro-Brownian thermal motions of molecular chain segments of PDLLA with the increase of HA particles.[33]

Based on the above results, a schematic model of hydrogen bonding between C═O groups in PDLLA and the surface P—OH groups in HA nanoparticle was designed as shown in Figure 6. The molecular chains of PDLLA polymer are random winding and prevent reversible phase from bringing irreversible strain that depends on the physical winding during inter-transition from glassy state to rubbery state.[51] However, in the nanocomposites the interpenetrating networks were formed due to a physical crosslinking by the hydrogen bonding, which served as a stationary phase during shape memory recovery, as shown in Figure 6. The model may also be used to explain the above results (e.g., the outcome from FTIR, DSC, and XPS).

Conclusions

HA nanoparticles were uniformly dispersed in PDLLA matrix in nanocomposites. The IR and XPS results showed that the hydrogen bonding between the C═O group of PDLLA and the surface P—OH group of HA (namely, P—O—H···O═C bonding) existed in PDLLA/HA nanocomposites. Moreover, the amount of hydrogen bonding increased as the addition of nano-HA particles increase. A schematic model of the hydrogen bondings was designed based on our analysis. On the contrary, the model also explained why better shape memory properties are achieved in the nanocomposites comparing with pure material. We hope that it is potential for the investigation on interface of polymer phase and inorganic nanoparticles phase.

Acknowledgment. This work was supported by Project 50303018 supported by National Natural Science Foundation of China.

CM0619398

(48) Lendlein, A.; Schmidt, A. M.; Schroeter, M.; Langer, R. *J. Polym. Sci. A* **2005**, *43*, 1369.
(49) Mohr, R.; Kratz, K.; Weigel, T.; Gabor, M. L.; Moneke, M.; Lendlein, A. *Proc. Natl. Acad. Sci.* **2006**, *103* (10), 3540.
(50) Ohki, T.; Ni, Q. Q.; Ohsako, N.; Iwamoto, M. *Composites, Part A* **2004**, *35*, 1065.
(51) Ferry, J. D. *Viscoelastic Properties of Polymers*; Wiley Press: New York, 1961.